

## Land-cover changes and microclimate risks around Yogyakarta International Airport

R. Muhammad Syarif Abdurrahman<sup>1</sup> ✉, R. Yosi Aprian Sari<sup>2</sup>.

<sup>1</sup>Department of Cartography and Remote Sensing, Faculty of Geography, Universitas Gadjah Mada, Yogyakarta, Indonesia

<sup>2</sup>Department of Physics Education, Faculty of Mathematics and Natural Sciences, Universitas Negeri Yogyakarta, Yogyakarta, Indonesia

### Article History

Received 12 October 2025

Accepted 28 October 2025

Published 31 May 2026

### Keywords

Google Earth Engine

Landsat 8

Land Transformation

Urban Heat Island

### Abstract

International airport infrastructure development triggers complex spatial transformations with implications for the balance of regional ecosystems. This study analyzes land-cover change dynamics, surface temperature distribution, vegetation conditions, and microclimate risk zones in the Yogyakarta International Airport (YIA) area using Landsat 8 imagery processed on the Google Earth Engine platform. Methods include Random Forest classification for land cover mapping, Land Surface Temperature (LST) analysis, Normalized Difference Vegetation Index (NDVI) extraction, and Vegetation Stress Index (VSI) compilation as ecological pressure indicators. Results show a 27.2% expansion of forest cover and a 30.4% reduction in water bodies during 2015–2024, contrasting with conventional urban sprawl theory. Surface temperature increased across all land cover classes except built-up areas, which decreased by 2.85°C, with Urban Heat Island formation extending to a radius of 5–7 km. Findings introduce green intensification as a novel reforestation pathway driven by the internalization of mitigation obligations within infrastructure project design. This phenomenon challenges conventional theoretical assumptions and extends existing forest transition frameworks to tropical infrastructure contexts.

**Contact** R. Muhammad Syarif Abdurrahman [rmuhammadsyarifabdurrahman@mail.ugm.ac.id](mailto:rmuhammadsyarifabdurrahman@mail.ugm.ac.id) Department of Cartography and Remote Sensing, Faculty of Geography, Universitas Gadjah Mada, Yogyakarta, Indonesia

This is an open-access article distributed under the terms of the Creative Commons Attribution-ShareAlike 4.0 International License (<https://creativecommons.org/licenses/by-sa/4.0/>).

## Introduction

Large-scale transportation infrastructure development is one of the most powerful drivers of contemporary landscape transformation. Globally, the expansion of aviation and highway networks has driven massive land-cover conversion across various ecological regimes: [Seto et al. \(2012\)](#) project that global urban land area will nearly triple between 2000 and 2030, with the greatest impact in tropical regions, which are also global biodiversity hotspots. International-scale infrastructure creates ecological influence zones extending to a radius of 15–20 km, encompassing modifications to the hydrological cycle, shifts in land-cover composition, and spatially detectable changes in microclimate ([Cidell, 2015; Liu et al., 2020](#)). The pressures on these ecosystems are multidimensional: in addition to direct land-cover conversion, there are thermal effects from large-scale impervious surfaces and habitat fragmentation, which cumulatively erode ecosystem services progressively ([McDonnell & Pickett, 1990; Lambin & Meyfroidt, 2011](#)). Advances in cloud-based remote sensing technology—particularly the Google Earth Engine (GEE) platform, which enables the efficient processing of high-resolution multitemporal satellite imagery at a regional scale—have revolutionized the capacity to monitor the ecological impacts of infrastructure development ([Gorelick et al., 2017](#)) and opened opportunities for systematic evaluations that were previously unfeasible.

Studies on the impact of transportation infrastructure development on land-cover transformation have yielded inconsistent findings in the literature. [Griffiths et al. \(2013\)](#) identified patterns of conventional urban sprawl around major transportation infrastructure in the Shanghai metropolitan area, with built-up areas expanding predominantly within a 10-km radius of infrastructure nodes. In contrast, [Zhang et al. \(2019\)](#) reported a re-greening phenomenon in several East Asian regions in response to increasingly stringent environmental regulations—a pattern known in [Meyfroidt & Lambin's \(2011\)](#) forest transition theory as the “state forest policy pathway,” where regulatory pressure drives reforestation regardless of market dynamics. This disparity in findings reflects the complexity of interactions between local regulatory contexts, geographic characteristics, and land-use policies. In the context of thermal analysis, [Li et al. \(2013\)](#) demonstrated that infrastructure with extensive impermeable surfaces creates localized heat islands with characteristics distinct from the conventional urban heat islands described by [Oke \(1987\)](#) based on the surface energy balance model. The inconsistency of these findings underscores that no single universal pattern can be predicted from transportation infrastructure development, and that a multi-indicator approach—combining analyses of land cover, surface temperature, and vegetation indices—is better able to capture the true complexity of ecological dynamics ([Pettorelli et al., 2005; Gorelick et al., 2017](#)).

Although studies on the environmental impacts of infrastructure have advanced significantly in temperate and subtropical regions, similar research in tropical regions—particularly Indonesia—remains very limited. This represents a significant gap: projections by [Seto et al. \(2012\)](#) indicate that tropical regions will experience the highest rate of urban expansion globally in the coming decades, while also being hotspots of biodiversity on Earth. Tropical characteristics such as dense vegetation cover, a dominant rainy season, and unique hydrological dynamics result in ecological transformation patterns that cannot be directly extrapolated from findings in other parts of the world ([Lambin & Meyfroidt, 2011](#)). This gap is critical given that Indonesia is entering an era of massive transportation infrastructure development. Without an adequate empirical basis for patterns of ecological transformation in the Indonesian tropical context, spatial planning policies and environmental mitigation strategies risk being off target. A fundamental unanswered question is: does airport infrastructure development in tropical Indonesia follow conventional urban sprawl patterns, or are there ecological mechanisms and policies that produce different transformation patterns?

Yogyakarta International Airport (YIA), which has been in operation since 2019, represents a strategic and unique case study for addressing this research gap. With an operational area of 587 hectares that converted productive agricultural land and coastal ecosystems in Kulon Progo Regency, YIA is one of Indonesia's new-generation international airports whose construction was accompanied by relatively strict environmental mitigation requirements, including obligations for reforestation programs and the establishment of conservation buffer zones ([Bappeda Kulon Progo, 2012](#)). YIA's location in a transitional zone between sandy coastal plains and irrigated agricultural land creates a distinctive physical context for the dynamics of tropical ecological transformation. The combination of a significant scale of development, a relatively robust regulatory framework, and a unique ecological context makes YIA an ideal natural laboratory for testing and expanding theories of landscape transformation driven by transportation infrastructure in a tropical context.

Based on the background and research gaps outlined above, this study aims to: (1) analyze the dynamics of land cover transformation in the YIA area during the 2015–2024 period using a GEE-based Random Forest classification; (2) examine the spatial distribution of land surface temperature (LST) and the characteristics of Urban Heat Island formation; (3) evaluate changes in vegetation conditions through NDVI analysis by land cover class; and (4) identify spatial ecological stress zones using the Vegetation Stress Index (VSI) as an integrative indicator. Collectively, these four objectives are designed to build a holistic understanding of environmental transformation patterns resulting from airport infrastructure development in a tropical context and provide an empirical basis for the development of evidence-based mitigation policies

## Method

This study employs a multitemporal spatial analysis approach that integrates remote sensing with cloud-based geospatial computing to detect changes in land cover, thermal conditions, and ecological pressure in the YIA area. All data processing was conducted using Google Earth Engine (GEE), which enables efficient analysis of regional-scale multispectral satellite imagery.

### Research Location and Time

The study is centered in the Yogyakarta International Airport (YIA) area, Kulon Progo Regency, with a study area defined as a circular buffer zone with a radius of 15 km from the airport's central point (7°54'S, 110°03'E), covering a total area of approximately 695.45 km<sup>2</sup> that includes parts of Kulon Progo, Bantul, and Purworejo Regencies. The 15-km radius was determined based on ICAO Annex 14 (2018) standards, which define the operational impact zone of an international airport as 13–17 km, as well as findings by [Cidell \(2015\)](#) indicating significant spatial impacts of airport development within a 10–20 km radius. Temporal analysis was conducted at two time points: 2015, the pre-construction baseline, and 2024, the post-operational condition. The year 2015 was selected because airport construction began in 2016, thereby representing natural conditions before large-scale anthropogenic intervention. This nine-year span meets the recommendations of [Chang et al. \(2018\)](#), which establish a minimum period of 7–10 years to detect significant spatial and ecological changes resulting from infrastructure development.

### Data and data source

The primary data for this study consist of Landsat 8 OLI/TIRS Collection 2 Level 2 satellite imagery accessed through the GEE catalog. Landsat 8 was selected based on its optimal combination of spectral (11 bands), temporal (16 days), and spatial (30 meters) resolutions, which are optimal for analyzing regional-scale land cover changes, with thermal infrared data quality (Bands 10–11) sufficient for LST estimation with a standard deviation of  $\pm 1.5^{\circ}\text{C}$  ([Jiménez-Muñoz et al., 2014](#)). Image selection used a maximum cloud-cover threshold of 10%, and the mosaicking process employed a median reducer function to minimize temporal noise and atmospheric

anomalies. Administrative boundary data were obtained from the National Geospatial Information Agency; all data were projected into the WGS 1984 UTM Zone 49S coordinate system.

Land cover classification was performed using the Random Forest algorithm with 100 decision trees and a maximum depth of 15. This algorithm was chosen for its ability to handle multidimensional data with high accuracy and resistance to overfitting (Breiman, 2001), having been shown to achieve 85–95% accuracy in classifying Landsat imagery (Rodríguez-Galiano et al., 2012). The classification scheme uses five classes, based on the Anderson Level I, adapted to Indonesian conditions: agricultural land, built-up areas, water bodies, open land, and forest. Training samples were generated through visual interpretation of imagery using high-resolution Google Earth imagery, resulting in 8,891 samples (2015) and 8,970 samples (2024). Accuracy validation using a confusion matrix with stratified random sampling yielded an Overall Accuracy of 84.2% (Kappa 0.79) for 2015 and 87.3% (Kappa 0.83) for 2024—values indicating very good agreement (Landis & Koch, 1977).

Analysis of Land Surface Temperature using the Single-Channel algorithm (Jiménez-Muñoz & Sobrino, 2003) with input from Landsat 8 Thermal Infrared Sensor Band 10. Surface emissivity correction using the NDVI-based emissivity estimation approach (Sobrino et al., 2004) with emissivity values ranging from 0.92 (urban surfaces) to 0.95 (dense vegetation). The Normalized Difference Vegetation Index (NDVI) was extracted using the standard Tucker formula (1979):  $NDVI = (NIR - Red) / (NIR + Red)$ , with input from Band 5 (NIR) and Band 4 (Red). Changes in NDVI were analyzed by land-cover class, in both absolute values and percentages, to assess vegetation degradation or recovery comparatively.

The Vegetation Stress Index (VSI) was developed as an integrative indicator that combines NDVI and LST, based on the premise that stressed vegetation exhibits low NDVI and high LST. The VSI formula uses z-score normalization:  $VSI = (0.5 \times LST_{norm}) - (0.5 \times NDVI_{norm})$ , where the mean ( $\mu$ ) and standard deviation ( $\sigma$ ) are calculated from the entire study area. Stress zone classification uses the 75th percentile threshold as the critical boundary; areas above the threshold are classified as high-stress zones. Temporal analysis of the VSI identifies new stress areas (transition from normal to high stress) and recovered areas (recovery from high stress to normal conditions).

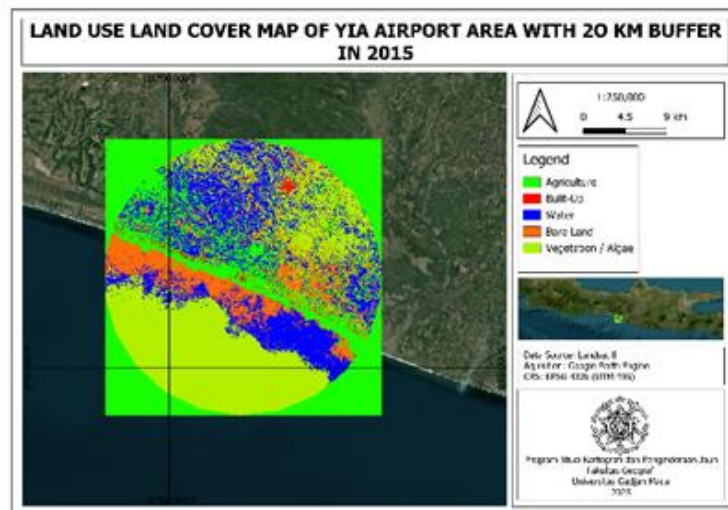
## Result

### Land Cover Change 2015–2024

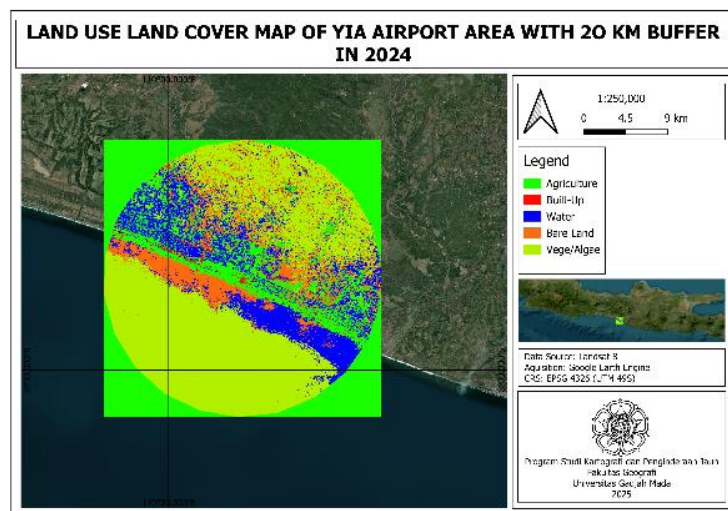
The Random Forest classification produced land-cover maps with overall accuracies of 84.2% (2015) and 87.3% (2024). The most notable changes during the 2015–2024 period were the expansion of forest areas by 80.36 km<sup>2</sup> (+27.2%) and the contraction of water bodies by 55.64 km<sup>2</sup> (–30.4%). Agricultural land decreased by 14.37 km<sup>2</sup> (–13.6%), while built-up areas and open land decreased by 0.85 km<sup>2</sup> and 9.53 km<sup>2</sup>, respectively (Table 1). The spatial distribution shows a concentric pattern, with the highest transformation intensity within a 0–5 km radius of the airport center (Fig 1).

Table 1. Changes in land cover area in the YIA region for the period 2015–2024

Land Cover Klass (km <sup>2</sup> )	Area 2015 (km <sup>2</sup> )	Area 2024 (km <sup>2</sup> )	Change (km <sup>2</sup> )	Change (%)
Agricultural Land	105,70	91,33	-14,37	-13,6
Built-up Area	6,76	5,91	-0,85	-12,6
Water Bodies	183,15	127,51	-55,64	-30,4
Open Land	104,86	95,33	-9,53	-9,1
Forests	295,00	375,36	+80,36	+27,2



(a)



(b)

Fig 1. Land cover distribution map of the YIA area for (a) 2015 and (b) 2024

### Soil Surface Temperature Distribution

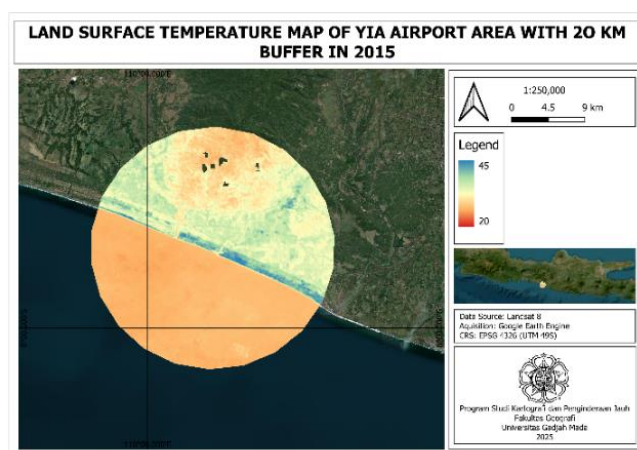
LST analysis shows an increase in temperature across all land cover classes except built-up areas, which experienced a decrease of 2.85°C—from 38.30°C (2015) to 35.45°C (2024). The highest temperature increases occurred in the forest class (+2.42°C) and water bodies (+2.20°C). Zones with extreme temperatures above 35°C are concentrated in the runway, apron, and taxiway areas, forming an Urban Heat Island that extends up to a radius of 5–7 km from the airport center with a distribution pattern that extends along the north–south runway orientation (Table 2, Figure 2).

### Changes in the Normalized Difference Vegetation Index (NDVI)

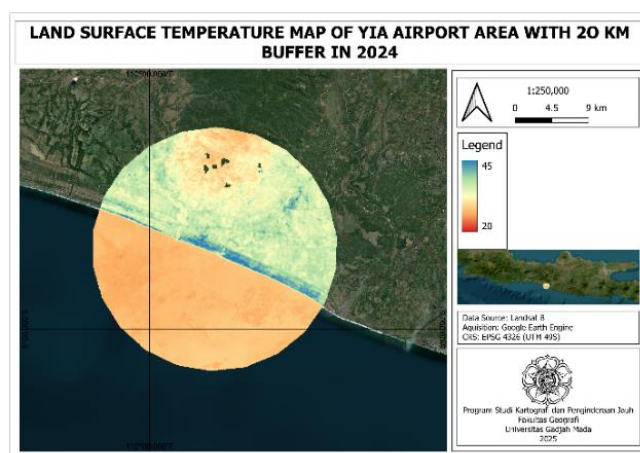
The most significant decline in NDVI occurred in agricultural land (−0.082 units; −12.29%) and forests (−0.069 units; −10.36%). In contrast, built-up areas showed an increase in NDVI of +0.082 units (+20.15%), while open land increased by +0.027 units (+4.24%). Water bodies experienced a moderate decrease of −0.044 units (−6.70%) (Table 3, Figure 3).

Table 2. Changes in Land Surface Temperature by land cover class for the period 2015–2024

Land Cover Class	LST 2015 (°C)	LST 2024 (°C)	Change (°C)
Agricultural Land	33,80	35,99	+2,19
Built-up Area	38,30	35,45	-2,85
Water Bodies	32,98	35,18	+2,20
Open Land	33,35	34,76	+1,41
Forests	32,99	35,41	+2,42



(a)

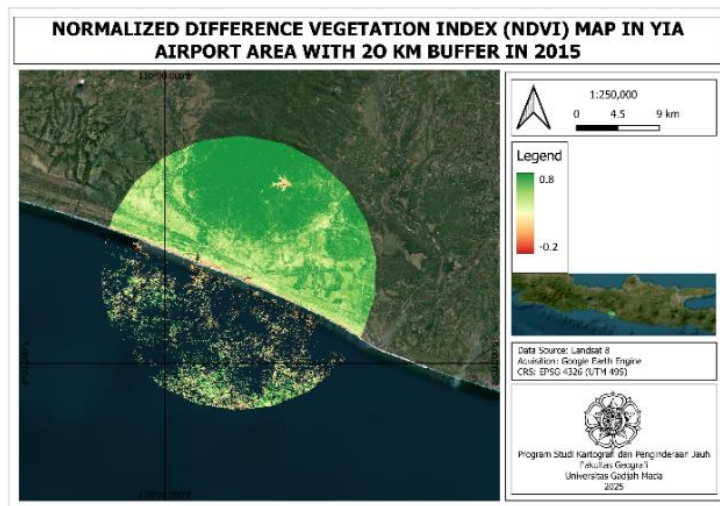


(b)

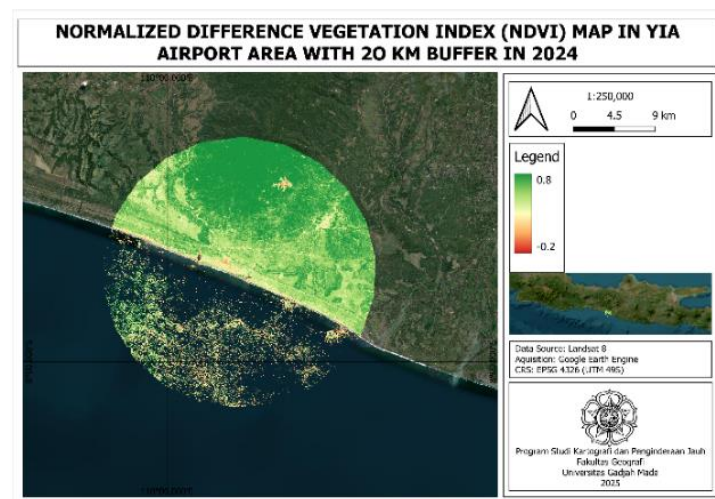
Fig 2. Changes in Land Surface Temperature by land cover class for the periods 2015 (a) and 2024 (b)

Table 3. Changes in the Normalized Difference Vegetation Index by land cover class for the period 2015–2024

Kand Cover Klass	NDVI 2015	NDVI 2024	Change	Change (%)
Agricultural Land	0,667	0,585	-0,082	-12,29
Built-up Area	0,407	0,489	+0,082	+20,15
Water Bodies	0,657	0,613	-0,044	-6,70
Open Land	0,637	0,664	+0,027	+4,24
Forests	0,666	0,597	-0,069	-10,36



(a)



(b)

Fig 3. Map showing the distribution of the Normalized Difference Vegetation Index (NDVI) for the YIA area in (a) 2015 and (b) 2024

### Dynamics of the Vegetation Stress Index

The VSI analysis identified a new stress area covering 11.52 km<sup>2</sup> (1.66% of the total study area) and a recovered area covering 16.98 km<sup>2</sup> (2.44%), resulting in a net recovery of +5.46 km<sup>2</sup> (+0.79%) (Table 4). The spatial distribution shows a concentration of high stress in a semicircular zone in the northern part of the YIA area, which correlates with zones of most intensive construction and land conversion (Fig 4).

Table 4. Results of the Vegetation Stress Index analysis for the YIA area for the period 2015–2024

Parameter VSI	Area (km <sup>2</sup> )	Percentage (%)
New Stress Area	11,52	1,66
Recovered Area	16,98	2,44
Net Recovery	+5,46	+0,79

Notes:

New Stress Area = an area that has experienced an increase in stress from normal conditions (2015) to high stress (2024).

Recovered Area = an area that has experienced a decrease in stress from high stress (2015) to normal/low stress (2024).

Net Recovery = the difference between Recovered and New Stress Areas; a positive value indicates an improvement in the ecosystem's overall condition.

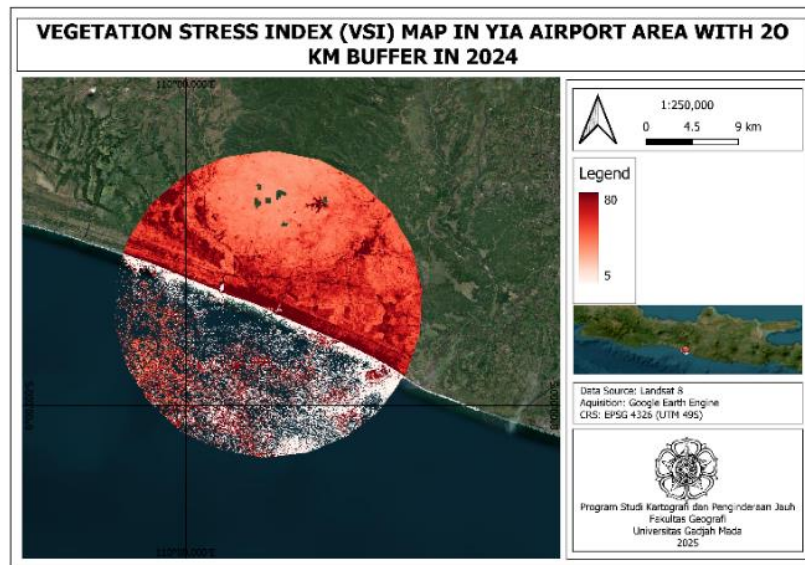


Fig 4. Map of the Vegetation Stress Index distribution in the YIA area in 2024

## Discussion

### *Green Intensification: A New Pathway in Forest Transition Theory*

Findings on land-cover transformation in the YIA area directly challenge the conventional urban-sprawl paradigm that dominates the literature on the impacts of transportation infrastructure. [Griffiths et al. \(2013\)](#) predicted that large-scale infrastructure development should trigger a dominant expansion of built-up areas, with vegetation being the primary victim of fragmentation. However, empirical data in the YIA area actually show an inverse pattern: forest expansion (+27.2%) occurred alongside a contraction of built-up areas (-12.6%) and relatively controlled agricultural conversion. This pattern extends beyond the partial re-greening phenomenon reported by [Zhang et al. \(2019\)](#) in East Asia.

Within the framework of the forest transition theory proposed by [Meyfroidt & Lambin \(2011\)](#), the pattern observed in YIA most closely resembles the state forest policy pathway—in which reforestation is driven by state regulatory intervention rather than by market forces or resource scarcity. However, what fundamentally distinguishes the YIA case is that this reforestation occurs alongside large-scale infrastructure development—a configuration not specifically documented in existing pathway classifications. We refer to this phenomenon as “green intensification”: a reorganization of vegetation cover driven not by reduced development pressure, but by mitigation obligations internalized within the development process itself. This study thus expands the framework of [Lambin & Meyfroidt \(2011\)](#) on land use transitions by identifying a new pathway—infrastructure-coupled green intensification—where environmental mitigation policies embedded in large infrastructure projects, rather than macroeconomic factors or resource scarcity, serve as the effective driver of reforestation in developing countries.

The mechanism behind this green intensification can be identified through three causal factors that operate synergistically. First, the environmental mitigation requirements inherent in the YIA project mandate reforestation programs and the establishment of conservation buffer zones, creating structural incentives for the expansion of vegetation cover ([Bappeda Kulon Progo, 2012](#)). Second, the concept of induced development proposed by [Cidell \(2015\)](#) explains that built-up activities tend to densify along major accessibility corridors outside the study radius, rather than spreading evenly across the buffer zone—thereby “freeing” the area within the buffer from direct development pressure. Third, as documented in land-use transition dynamics across various developing countries ([Lambin & Meyfroidt, 2011](#)), shifts in local economic patterns from subsistence agriculture to the service sector drive land abandonment, which subsequently triggers natural vegetation succession into secondary forests. The theoretical implication of this finding is that the urban sprawl paradigm cannot serve as a universal framework for predicting the impacts of transportation infrastructure, particularly in the context of relatively strong environmental regulations.

### ***Thermal Anomalies: The Mechanisms Behind Temperature Declines in Built-Up Areas***

The 2.85°C decrease in LST in built-up areas is an anomaly that cannot be explained by conventional Urban Heat Island theory. Based on the surface energy balance model developed by [Oke \(1987\)](#), the expansion of impermeable surfaces with high specific heat capacity (concrete and asphalt) and low albedo should consistently increase sensible heat flux and surface temperature. Li et al. (2013) confirmed this mechanism in the context of transportation infrastructure in Shanghai, where areas with high impermeable surface density consistently exhibited higher LSTs than surrounding areas. This anomaly thus demands an explanation that goes beyond the predictions of conventional theory.

The key to explaining this anomaly lies in the fundamental changes in the composition of built-up areas between 2015 and 2024. In 2015, the built-up category was dominated by traditional rural settlements with clay tile roofs (high emissivity, low albedo of approximately 0.10–0.20) and unstructured yard vegetation. By 2024, YIA airport infrastructure dominated this category with three qualitatively distinct thermal characteristics: (1) reflective roofing materials with high albedo (0.65–0.85) that reduce solar radiation absorption – [Santamouris \(2014\)](#) demonstrates that every 0.1 increase in roof reflectivity can lower the average urban ambient temperature by 0.2 K; (2) natural ventilation systems in terminal designs that minimize anthropogenic heat emissions; and (3) the integration of structured green open spaces that function as active evapotranspiration sinks. The combination of these three characteristics—which constitute the implementation of green airport design principles—collectively shifts the thermal profile of the built area toward a cooler state compared to the baseline of traditional settlements. These findings extend [Santamouris's \(2014\)](#) review to the context of airport infrastructure in tropical regions and have important implications for future infrastructure design: integrated green building design is not merely an aesthetic strategy or a means of fulfilling regulatory obligations, but rather an empirically measurable mechanism for microclimate mitigation.

### ***The Paradox of Forest Expansion and NDVI Decline: The Forest Age Effect in Tropical Regions***

The most significant paradox in this study is the 10.36% decrease in the average NDVI of forest classes despite a 27.2% increase in forest cover area. This paradox can be explained by understanding the dynamics of vegetation succession and the spectral characteristics of young secondary forests compared to mature forests—a challenge known in the remote sensing literature as the NDVI saturation problem ([Pettorelli et al., 2005](#)).

Forest expansion in the YIA area is dominated by active reforestation and natural succession on abandoned agricultural land. Early-succession vegetation has a sparse canopy, an unconsolidated stand structure, and a leaf area index (LAI) that is significantly lower than that of mature forests. As demonstrated by [Pettorelli et al. \(2005\)](#), NDVI responds nonlinearly to increases in vegetation density and reaches saturation at values around 0.7–0.9—a value achieved only by mature forests with closed canopies—while early-succession vegetation has NDVI values ranging from 0.3 to 0.5. When extensive areas of young forest are grouped with mature forest into a single classification class, the aggregate average NDVI value of the forest class decreases even though its area increases. This phenomenon is analogous to the forest age effect in studies of secondary forest dynamics, where Net Primary Production and biomass content in young secondary forests can be only 50–70% of those in mature forests during the first 10–20 years of regeneration ([Meyfroidt & Lambin, 2011](#)). This study represents the first documentation of this phenomenon in the context of airport infrastructure development in tropical regions.

These findings have critical methodological implications: an increase in forest cover based on LULC analysis should not be interpreted as an automatic improvement in ecosystem quality. As [Meyfroidt & Lambin \(2011\)](#) noted, a reduction in deforestation pressure does not in itself account for differences in ecological quality between old-growth forests and young secondary forests. A valid environmental impact assessment requires a multi-indicator approach that considers not only the extent of land cover (LULC), but also vegetation maturity (NDVI) and the ecological stress it faces (VSI). The LULC-LST-NDVI-VSI analytical framework developed in this study directly addresses these methodological needs and can serve as a model for evaluating reforestation programs in other infrastructure areas.

### ***Scientific Contributions and Theoretical Implications***

In the context of land change science, this study provides empirical evidence of green intensification triggered by airport infrastructure development in tropical Indonesia—a phenomenon previously undocumented in the literature. This finding directly expands the forest transition theory framework of [Meyfroidt & Lambin \(2011\)](#) by identifying a new pathway: infrastructure-coupled green intensification—in which reforestation and infrastructure development occur simultaneously through the internalization of mitigation obligations into project design. This differs fundamentally from the five pathways in the [Meyfroidt & Lambin \(2011\)](#) classification, as it is not pre-development conditions that drive reforestation, but rather the development requirements themselves.

Methodologically, the developed LULC-LST-NDVI-VSI multi-indicator analytical framework has proven capable of revealing anomalies and paradoxes that would not be detected through single-variable analysis. VSI's capability as an integrative indicator, sensitive to the combined effects of thermal and vegetation stressors, provides greater diagnostic precision for identifying ecological stress zones. Implementation of the entire framework in GEE—described by [Gorelick et al. \(2017\)](#) as a platform that enables open-source geospatial analysis at a planetary scale—enables replication in other regions with limited computational infrastructure. This is particularly relevant for developing countries, which, according to projections by [Seto et al. \(2012\)](#), will experience the highest rates of urban and infrastructure expansion globally in the coming decades, yet often have limited environmental monitoring resources. In the context of remote sensing studies, this research demonstrates the value of distinguishing between changes in land use and land cover (LULC) and changes in vegetation quality (NDVI) as two evaluation dimensions that are not interchangeable.

## Conclusion

This study demonstrates that the relationship between large-scale infrastructure development and environmental dynamics is far more complex than conventional theory predicts. Rather than resulting in linear land-cover degradation as suggested by the urban sprawl paradigm, the development of YIA triggers a paradoxical spatial reorganization: green intensification occurs alongside localized ecological pressures, and modern infrastructure actually produces a cooler thermal profile than the traditional settlements it replaces. Collectively, these findings confirm that the urban sprawl paradigm cannot serve as a universal framework for predicting the environmental impacts of transportation infrastructure, particularly in tropical regions with distinctive regulatory and ecological dynamics. Theoretically, the concept of green intensification documented in this study represents a mechanism distinct from passive re-greening: it constitutes an active ecological response to mitigation policies internalized within infrastructure design and management. This phenomenon expands Meyfroidt & Lambin's (2011) forest transition theory by identifying a new pathway that does not require a reduction in development pressure as a prerequisite. The identified paradox of forest expansion–NDVI decline also underscores that the quantity and quality of vegetation cover are two distinct dimensions of evaluation that cannot substitute for one another in assessing ecosystem conditions.

In practical terms, this study has direct implications for infrastructure planning: strict environmental mitigation standards, green airport designs based on thermal principles, and reforestation programs that account for vegetation maturity—rather than merely the area of coverage—have been shown to yield better ecological outcomes. These findings support integrating environmental standards into the permitting and evaluation processes for infrastructure projects as a long-term investment in ecosystem resilience, rather than merely a regulatory obligation. Future research should develop machine learning-based predictive models capable of projecting patterns of land-cover transformation and ecological pressures 5–10 years after infrastructure becomes operational under different policy scenarios. Expanding the analysis to biodiversity and ecosystem services is urgently needed: Seto et al. (2012) warn that the rate of urban expansion in tropical regions—which are biodiversity hotspots—will result in disproportionate habitat loss compared to other regions—an implication relevant to the area surrounding YIA, which lies within the southern Java coastal ecological corridor. An evaluation of the replicability of the LULC-LST-NDVI-VSI framework in other international airport cases in Indonesia and the ASEAN region will also strengthen the generalizability of these findings and support the development of context-specific environmental monitoring standards for infrastructure in tropical regions.

## Acknowledgement

The authors would like to thank the committee of the IV Geography Seminar at Gadjah Mada University for the opportunity to present the results of this research, which serves as the basis for developing the article into a scientific publication. External funding sources do not fund this research.

## Author Contribution

Conceptualization, R.M.S. Abdurrahman and R.Y.A. Sari; Methodology, R.M.S. Abdurrahman; Data Curation, R.M.S. Abdurrahman; Formal Analysis, R.M.S. Abdurrahman and R.Y.A. Sari; Investigation, R.M.S. Abdurrahman; Spatial Analysis and Visualization, R.M.S. Abdurrahman; Writing—Original Draft Preparation, R.M.S. Abdurrahman; Writing—Review and Editing, R.Y.A. Sari; Supervision, R.Y.A. Sari. All authors have read and agreed to the published version of the manuscript.

### Data Availability

All data generated or analyzed during this study are presented in the tables and figures within this article.

### Funding

This research received no external funding.

### Conflict of Interest

The authors declare that they have no known competing financial interests or personal relationships that could have influenced the work reported in this paper.

### References

- Arjasakusuma, S., Kamal, M., Hafizt, M., & Forestriko, H. F. (2018). Local-scale accuracy assessment of vegetation cover change maps derived from Global Forest Change data, ClasLite, and supervised classifications: case study in part of Riau Province, Indonesia. *Applied Geomatics*, 10(3), 205–217. <https://doi.org/10.1007/s12518-018-0215-4>
- Badan Perencanaan Pembangunan Daerah Kabupaten Kulon Progo. (2012). Rencana Tata Ruang Wilayah Kabupaten Kulon Progo 2012–2032. Wates: Bappeda Kulon Progo.
- Breiman, L. (2001). Random forests. *Machine Learning*, 45(1), 5–32. <https://doi.org/10.1023/A:1010933404324>
- Chang, Y., Hou, K., Li, X., Zhang, Y., & Chen, P. (2018). Review of progress in land use and land cover change research. *IOP Conference Series: Earth and Environmental Science*, 113, 012087. <https://doi.org/10.1088/1755-1315/113/1/012087>
- Cidell, J. (2015). The role of major infrastructure in suburban development: an empirical study of airports and highways. *Journal of Transport Geography*, 44, 44–53. <https://doi.org/10.1016/j.jtrangeo.2015.02.012>
- Gorelick, N., Hancher, M., Dixon, M., Ilyushchenko, S., Thau, D., & Moore, R. (2017). Google Earth Engine: Planetary-scale geospatial analysis for everyone. *Remote Sensing of Environment*, 202, 18–27. <https://doi.org/10.1016/j.rse.2017.06.031>
- Griffiths, P., Hostert, P., Gruebner, O., & van der Linden, S. (2013). Mapping megacity growth with multi-sensor data. *Remote Sensing of Environment*, 136, 450–465. <https://doi.org/10.1016/j.rse.2013.05.023>
- International Civil Aviation Organization. (2018). Annex 14 to the Convention on International Civil Aviation: Aerodromes, Volume I (8th ed.). Montreal: ICAO.
- Jiménez-Muñoz, J. C., & Sobrino, J. A. (2003). A generalized single-channel method for retrieving land surface temperature from remote sensing data. *Journal of Geophysical Research: Atmospheres*, 108(D22), 4688. <https://doi.org/10.1029/2003JD003480>
- Jiménez-Muñoz, J. C., Sobrino, J. A., Skoković, D., Mattar, C., & Cristóbal, J. (2014). Land surface temperature retrieval methods from Landsat-8 thermal infrared sensor data. *IEEE Geoscience*

- and Remote Sensing Letters, 11(10), 1840–1843.  
<https://doi.org/10.1109/LGRS.2014.2312032>
- Khoirurrizqi, Y., Sasongko, R., Utami, N. L. E., Irbah, A., & Arjasakusuma, S. (2023). Machine Learning-Based Rice Field Mapping in Kulon Progo using a Fusion of Multispectral and SAR Imagery. *Forum Geografi*, 37(2), 134–148. <https://doi.org/10.23917/forgeo.v37i2.20304>
- Lambin, E. F., & Meyfroidt, P. (2011). Global land-use change, economic globalization, and looming land scarcity. *Proceedings of the National Academy of Sciences*, 108(9), 3465–3472. <https://doi.org/10.1073/pnas.1100480108>
- Landis, J. R., & Koch, G. G. (1977). The measurement of observer agreement for categorical data. *Biometrics*, 33(1), 159–174. <https://doi.org/10.2307/2529310>
- Li, J., Song, C., Cao, L., Zhu, F., Meng, X., & Wu, J. (2013). Impacts of landscape structure on surface urban heat islands: A case study of Shanghai, China. *Remote Sensing of Environment*, 115(12), 3249–3263. <https://doi.org/10.1016/j.rse.2011.07.008>
- Liu, Y., Song, W., & Deng, X. (2020). Understanding the spatiotemporal variation of urban land expansion in oasis cities by integrating remote sensing and multi-dimensional DPSIR-based indicators. *Ecological Indicators*, 96, 23–37. <https://doi.org/10.1016/j.ecolind.2018.01.029>
- McDonnell, M. J., & Pickett, S. T. A. (1990). Ecosystem structure and function along urban-rural gradients: an unexploited opportunity for ecology. *Ecology*, 71(4), 1232–1237. <https://doi.org/10.2307/1938259>
- Meyfroidt, P., & Lambin, E. F. (2011). Global forest transition: Prospects for an end to deforestation. *Annual Review of Environment and Resources*, 36, 343–371. <https://doi.org/10.1146/annurev-enviro-090710-143732>
- Oke, T. R. (1987). *Boundary Layer Climates* (2nd ed.). Routledge. <https://doi.org/10.4324/9780203407219>
- Pettorelli, N., Vik, J. O., Mysterud, A., Gaillard, J. M., Tucker, C. J., & Stenseth, N. C. (2005). Using the satellite-derived NDVI to assess ecological responses to environmental change. *Trends in Ecology & Evolution*, 20(9), 503–510. <https://doi.org/10.1016/j.tree.2005.05.011>
- Rodriguez-Galiano, V. F., Ghimire, B., Rogan, J., Chica-Olmo, M., & Rigol-Sanchez, J. P. (2012). An assessment of the effectiveness of a random forest classifier for land-cover classification. *ISPRS Journal of Photogrammetry and Remote Sensing*, 67, 93–104. <https://doi.org/10.1016/j.isprsjprs.2011.11.002>
- Roy, D. P., Wulder, M. A., Loveland, T. R., Woodcock, C. E., Allen, R. G., Anderson, M. C., ... & Scambos, T. A. (2014). Landsat-8: Science and product vision for terrestrial global change research. *Remote Sensing of Environment*, 145, 154–172. <https://doi.org/10.1016/j.rse.2014.02.001>
- Santamouris, M. (2014). Cooling the cities: A review of reflective and green roof mitigation technologies to fight heat island and improve comfort in urban environments. *Solar Energy*, 103, 682–703. <https://doi.org/10.1016/j.solener.2012.09.003>

- Seto, K. C., Güneralp, B., & Hutyra, L. R. (2012). Global forecasts of urban expansion to 2030 and direct impacts on biodiversity and carbon pools. *Proceedings of the National Academy of Sciences*, 109(40), 16083–16088. <https://doi.org/10.1073/pnas.1211658109>
- Sobrino, J. A., Jiménez-Muñoz, J. C., & Paolini, L. (2004). Land surface temperature retrieval from LANDSAT TM 5. *Remote Sensing of Environment*, 90(4), 434–440. <https://doi.org/10.1016/j.rse.2004.02.003>
- Tucker, C. J. (1979). Red and photographic infrared linear combinations for monitoring vegetation. *Remote Sensing of Environment*, 8(2), 127–150. [https://doi.org/10.1016/0034-4257\(79\)90013-0](https://doi.org/10.1016/0034-4257(79)90013-0)
- Zhang, H., Qi, Z., Ye, X., Cai, Y., Ma, W., & Chen, M. (2019). Analysis of land use/land cover change, population shift, and their effects on spatiotemporal patterns of urban heat islands in metropolitan Shanghai, China. *Applied Geography*, 115, 102138. <https://doi.org/10.1016/j.apgeog.2019.102138>
- Zhang, X., Liu, L., Chen, X., Gao, Y., Xie, S., & Mi, J. (2020). GLC\_FCS30: global land-cover product with fine classification system at 30 m using time-series Landsat imagery. *Earth System Science Data*, 12(2), 1203–1219. <https://doi.org/10.5194/essd-12-1203-2020>